Aalborg Universitet

AALBORG UNIVERSITY
DENMARK

A Multiagent-based Consensus Algorithm for Distributed Coordinated Control of Distributed Generators in the Energy Internet

Sun, Qiuye; Han, Renke; Zhang, Huaguang; Zhou, Jianguo; Guerrero, Josep M.

A Multi-Agent-based Consensus Algorithm for Distributed Coordinated Control of Distributed Generators in the Energy Internet

Qiuye Sun, *Member, IEEE*, Renke Han[*], Huaguang Zhang, *Fellow, IEEE*, Jianguo Zhou, and Josep M. Guerrero, *Fellow, IEEE*

Abstract—With the bidirectional power flow provided by the Energy Internet, various methods are promoted to improve and increase the energy utilization between Energy Internet and Main-Grid. This paper proposes a novel distributed coordinated controller combined with a multi-agent-based consensus algorithm which is applied to distributed generators in the Energy Internet. Then, the decomposed tasks, models, and information flow of the proposed method are analyzed. The proposed coordinated controller installed between the Energy Internet and the Main-Grid keeps voltage angles and amplitudes consensus while providing accurate power-sharing and minimizing circulating currents. Finally, the Energy Internet can be integrated into the Main-Grid seamlessly if necessary. Hence the Energy Internet can be operated as a spinning reserve system. Simulation results are provided to show the effectiveness of the proposed controller in an Energy Internet.

Index Terms—Energy internet, distributed coordinated control, spinning reserve, multi-agent consensus algorithm, distributed generators (DGs)

NOMENCLATURE

I_a	active circulating current
I_r	reactive circulating current
ΔI	total circulating current
i	number of distributed generators (DGs)
δ_i	angle of voltage from DG
ω_i	the angular velocity of DG to represent the frequency
v_{odi}	d-axis output voltage components for DG
v_{oqi}	q-axis output voltage components for DG
i_{odi}	d-axis output voltage components for DG
i_{oqi}	q-axis output current components for DG
P_i	average active power for DG
Q_i	average reactive power for DG
ω_{ci}	cutoff frequency of power filter
m_i	angle-active droop parameter for DG
n_i	voltage-reactive droop parameter for DG
δ_{seti}	set value of angle-active droop control for DG
v_{seti}	set value of voltage-reactive droop control for DG
δ_i^*	reference of voltage angle for DG
v_{odi}^*	d-axis reference of voltage amplitude in the voltage controller for DG
v_{oqi}^*	q-axis reference of voltage amplitude in the voltage controller for DG
ϕ_{odi}	d-axis auxiliary state variables in the voltage controller for DG
ϕ_{oqi}	q-axis auxiliary state variables in the voltage controller for DG
F	feedforward parameter in the voltage controller
C_{fi}	filter capacitor for DG
i_{ldi}^*	d-axis current reference in the current controller for DG
i_{lqi}^*	q-axis current reference in the current controller for DG
k_{pVodi}	d-axis proportion parameters in the voltage controller for DG
k_{qVodi}	q-axis proportion parameters in the voltage controller for DG
k_{iVodi}	d-axis integral parameters in the voltage controller for DG
k_{iVoqi}	q-axis integral parameters in the voltage controller for DG
γ_{di}	d-axis auxiliary state variables in the current controller for DG
γ_{qi}	q-axis auxiliary state variables in the current controller for DG
i_{ldi}	d-axis filter current components for DG
i_{lqi}	q-axis filter current components for DG
v_{idi}^*	d-axis output of current controller for DG
v_{iqi}^*	q-axis output of current controller for DG
L_{fi}	filter inductance for DG
k_{pildi}	d-axis proportion parameters in the current controller for DG
k_{pilqi}	q-axis proportion parameters in the current controller for DG
k_{pildi}	d-axis integral parameters in the current controller for DG
k_{iilqi}	q-axis integral parameters in the current controller for DG
θ_{park}	Angle used for Park transformation

Q. Sun, R. Han, H, Zhang, and J. Zhou are with the School of Information Science and Engineering, Northeastern University, Shenyang 110819, China (sunqiuye@ise.neu.edu.cn, hanrenke.neu@gmail.com, zhanghuaguang@ise.neu.edu.cn, jianguozhou.neu@gmail.com)
J. M. Guerrero is with the Institute of Energy Technology, Aalborg University, Aalborg 9220, Denmark (Joz@et.aau.dk)
[*]Corresponding author (Renke Han). Tel: +86 024 83683907; fax: +86 024 83689605; E-mail address: hanrenke.neu@gmail.com

I. INTRODUCTION

WITH the large penetration of renewable energy in power systems, flexible energy management and power sharing among different distributed generators (DGs) have raised a major concern. Therefore, the concept of "Energy Internet", motivated by the Internet, has been proposed recently [1] and can provide promising solutions. Previous literatures about Energy Internet mainly focused on its architecture, system integration, and control of the solid-state transformer [2] [3]. However, in order to realize the envisioned Energy Internet conception, the critical design and control objectives should be considered: (1) maintaining flexible and proportional power-sharing among DGs; (2) maintaining system continuous synchronization with the Main-Grid considering load variations; (3) minimizing circulating currents between DGs, *iv*) achieving seamless energy transitions between Energy Internet and Main-Grid if necessary.

To realize proportional power-sharing among DGs in the Energy Internet, various control schemes have been proposed. The most important one is the droop control [4], an attractive distributed control scheme that has been widely studied recently since its operation does not require for high-bandwidth communication systems. In addition, a power sharing unit (PSU) is proposed to achieve power management strategy in a hybrid microgrid architecture in [5]. However, the conventional droop controller has several drawbacks such as load-dependent frequencies and voltage amplitudes, large circulating currents among DGs [6], the tradeoff between power-sharing accuracy and voltage synchronization [7] [8]. To overcome these shortcomings, a modified droop control strategy [9] has been proposed to improve the power-sharing accuracy considering the line-impedance effect through designing a proper virtual impedance. To restore the voltage and frequency of DGs to nominal values, the so-called secondary control has been recently investigated in the literature [10] [11], which demonstrate that proper communication systems are necessary to realize the control goals. The secondary control can be classified into centralized control and distributed control in general. The centralized control [12] [13]requires a central unit to receive all the information and to broadcast the decisions. Due to the centralized nature, it presents a single point failure which can reduce the reliability and stability of the whole system. Alternatively, the multi-agent system as a kind of distributed control structure has drawn much attention due to its flexibility and computational efficiency [14] [15]. In [16], the participation of a multi-agent-system-based microgrid into the Energy Market is proposed. In order to charge electric vehicles (EVs) at low electricity prices, an agent-based control system that coordinates the battery charging of electric vehicles in distribution networks is presented in [17]. In [18], the multi-agent system for EV charging control is proposed based on the Nash Certainty Equivalence in order to solve the grid impact. Meanwhile, the multi-agent consensus algorithm has been applied into control system based on the multi-agent system structure [19] [20]. However, these applications only solved a single problem of voltage restoration or frequency restoration. Furthermore, Energy Internet always suffers from large circulating currents caused by the slight differences among phases and amplitudes of the output voltages [21], which cannot be eliminated only by maintaining the synchronization of the output voltage angles or amplitudes.

In order to overcome the aforementioned challenges, this paper proposes a novel distributed coordinated controller combined with the multi-agent-based consensus algorithm to control DGs in the Energy Internet. Two main control objectives are achieved by the proposed control scheme: *i*) keep angles and amplitudes of all DGs' output voltages being synchronized with the Main-Grid information (restore to their nominal values), while keeping accurate proportional power-sharing; *ii*) eliminate (minimize) circulating currents among DGs in the Energy Internet. Specifically, *P*-δ and *Q*-*V* droop controls are adopted to suppress the circulating currents, while achieving proportional power-sharing. This can be achieved by regulating both the angles (δ) and amplitudes (V) at the same time. Due to the nonlinear feature of DGs in the Energy Internet, the proposed control approach is designed based on the input-output feedback linearization control principle [22] and related stability analysis approach [23].

The main features and benefits of the proposed controller are given as follows: (1) the structure of the proposed controller related to the conception of the multi-agent system is proposed including tasks decomposition, types of agents and information flow; (2) the novel distributed coordinated controller combined with the multi-agent consensus algorithm is proposed to control DGs in the Energy Internet; (3) the power can be shared in proportional and the angles and amplitudes of output voltages can be synchronized with the Main-Grid; (4) the circulating currents among DGs can be suppressed effectively; (5) the control method requires only a sparse communication structure which means each DG only needs its local information and its neighbor's information to achieve control objectives, then the controller can be more reliable and less expensive.

It is worthwhile to remark here that the proposed controller can bring extra benefits: (1) Energy Internet can be operated as a spinning reserve system when the leader information is from Main-Grid, then it can achieve seamless integration into Main-Grid; roughly speaking, the spinning reserve means that the bidirectional power flow between Energy Internet and Main-Grid could respond voluntarily to load disturbances within a given period of time [24] [25]; (2) facilitated by this advanced control and communication scheme, Energy Internet can provide opportunities to other smart end users (flexible loads such as Intelligence Data Centers) in our daily lives to satisfy the needs of their power demands while minimizing their energy cost [26]; (3) the system can supply other ancillary services such as market participation as well required by Main-Grid [27] [28]; (4) with the increasing number of renewable sources and the development of Energy Internet, the fuel crisis and environmental problems can be solved gradually.

This paper is organized as follows. In Section II, the architecture of the proposed controller based on multi-agent system is presented; the conception of different agents and information flow among agents are described. In Section III, the dynamic model of the single-inverter-based DG is established. Section IV discusses the distributed coordinated

controller designed by the input-output feedback linearization and the multi-agent consensus algorithm. In Section V, simulation results verify the effectiveness of the proposed controller. In Section VI, the comparisons of proposed distributed approach versus centralized approach are illustrated. Section VII concludes the paper. Section VIII illustrates the future work.

II. THE ARCHITECTURE OF THE DISTRIBUTED COORDINATED CONTROL BASED ON MULTI-AGENT SYSTEM

A. Requirements of the Proposed Distributed Coordinated Control

In order to achieve voltage synchronization, proportional power-sharing and spinning reserve requirements for Energy Internet, the distributed coordinated controller combined with multi-agent consensus algorithm is proposed. A typical architecture of Energy Internet integrated with the proposed controller is shown in Fig. 1. The energy sources in an Energy Internet consist of distributed renewable energy resources (DRERs), distributed energy storage devices (DESDs), Main-Grid (MG). In this paper, the designation of the controller structure used in an Energy Internet is based on the multi-agent system structure [29] [30] [31]and each DRER, DESD, MG is controlled by each different agent taking advantages of the autonomous, intelligent, cooperative proactive and adaptive features of the multi-agent system.
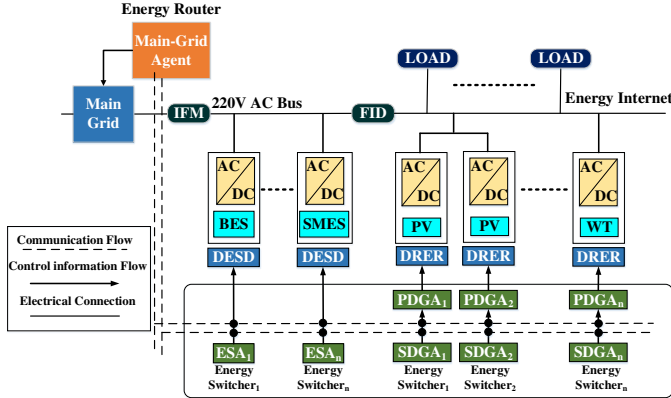

Fig. 1. Architecture of the Energy Internet

The proposed Energy Internet structure and distributed coordinated controller should meet the following requirements:

1) Achieve power-sharing in proportional among different DGs dynamically and restore the amplitudes and angles of output voltages to nominal value to keep tracking with the information from the leader (Main-Grid or one DG).

2) Ensure the high reliability of the proposed algorithm and maintain seamless transition when Energy Internet switches between the grid-connected mode and islanded mode, which is called spinning reserve condition.

3) Minimize the circulating current between different DGs to enhance efficiency of energy transmission.

4) Achieve sparse communication structure to enhance the reliability and efficiency of the control system.

B. Definitions of Agents

Each agent in the proposed controller has its own goals and functions. According to different goals and functions, there are three different agents designed for the distributed coordinated controller and two additional agents in the normal multi-agent system. The three different agents include the Main-Grid Agent (MGA), the DG Agents (DGAs) which consist of the Primary-DGA (PDGA) and the Secondary-DGA (SDGA), the Energy Storage Agents (ESAs). The MGA is also called energy router which is used to regulate the power flow between Energy Internet and Main-Grid. The ESA and SDGA are all called energy switcher which is used to regulate the power flow inside Energy Internet. The other two necessary agents in a multi-agent system include the agent management service agent (AMSA) which is compulsory and the directory facilitator agent (DFA) [29]. In addition, the intelligent fault management (IFM), and fault isolation device (FID) are also installed on the transition lines, whose functions are not discussed in this paper. The reference architecture of multi-agent system is shown in Fig. 2.
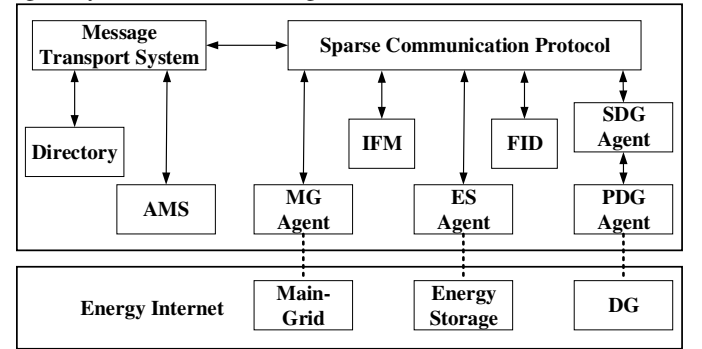

Fig. 2. Reference architecture of multi-agent system

1) Main-Grid Agent (MGA): In this paper, it is mainly used to choose the operation modes (grid-connected mode or islanded mode) for Energy Internet and calculate circulating currents between Main-Grid and Energy Internet. It provides the control information for the ESA and DGA. The general architecture of MGA is illustrated in Fig. 3.
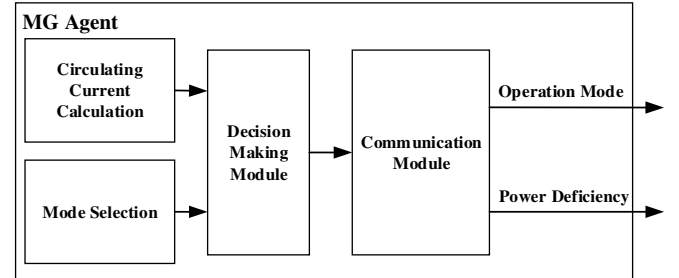

Fig. 3. Architecture of MGA

2) DG Agent (DGA): It consists of two sub-agent called Primary-DGA (PDGA) and the Secondary-DGA (SDGA) respectively. The PDGA is used to achieve local control objectives for each DG and the SDGA is used to achieve the distributed coordinated control between different DGs. The general architecture of DGA is illustrated in Fig. 4.

3) Energy Storage Agent (ESA): It is used to control the energy storage to compensate the power unbalance timely by which the control system can provide enough time for DGA to response to the load disturbance. The architecture of ESA is shown in Fig. 5.

4) Agent Management Service Agent (AMSA): It acts as a white page, maintaining a directory of agents registered within the control system.

5) Directory Facilitator Agent (DFA): It acts as a yellow page, maintaining a directory of agents and the services they can offer other agents.

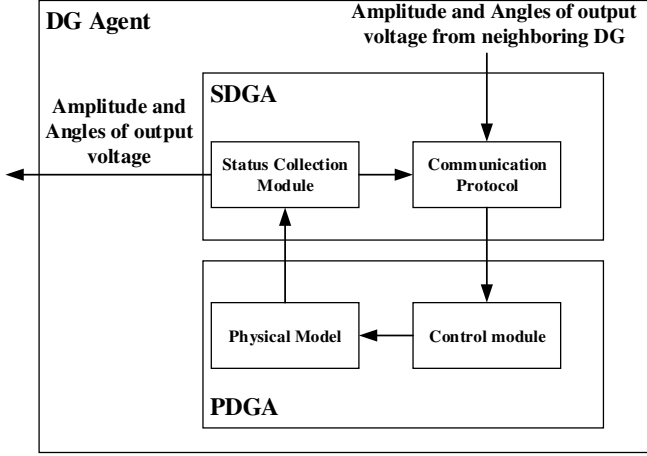The general architectures of AMSA and DFA are illustrated in [29] and [30].
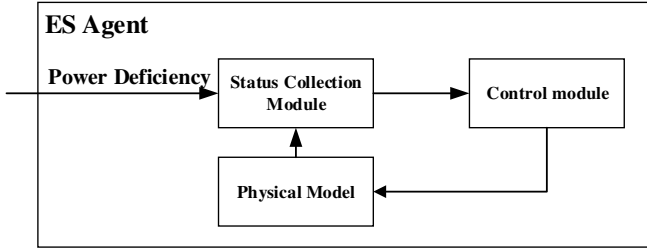

Fig. 4. Architecture of DGA

Fig. 5. Architecture of ESA

C. Implementation of Proposed Distributed Coordinated Control

Energy Internet can be operated under two modes. The first mode is that Energy Internet has no responsibility to connect with Main-Grid and can be operated in the isolated mode. In this mode, one of the DGs should be chosen as the leader in the control system. In addition, the leader DG should be controlled to output rated power in order to guarantee its leader information with a constant and normal value. The second mode is that Energy Internet should be connected to the Main-Grid if necessary; the information from Main-Grid should be as the leader information. In this mode, Energy Internet can be operated under the spinning reserve condition with bidirectional power flow to compensate the power disturbance in both Main-Grid and Energy Internet. The main difference between the two modes is whether Energy Internet should be connected with the Main-Grid. Except for that, other operations of the proposed controller of Energy Internet are same.

Fig. 6 illustrates the flowchart of the proposed controller combined with the algorithms, task decomposition and information flow required for the control system.

Step 1) Energy Internet confirms the operation modes. If Energy Internet is operated under the first mode, the MGA should choose one DG as the leader in the system. If Energy Internet should be operated under the second mode, the leader's information should be detected from the Main-Grid. Meanwhile, the active and reactive circulating current in Energy Internet should be calculated according to the equation

(2) and (3). If I_a or I_r suppress the standard value I_{anorm} or I_{rnorm}, other agents will be activated to implement their tasks.

Step 2) The large circulating current caused by the power unbalance means the big deviations of amplitudes and angles of voltages among DGs in Energy Internet. In order to compensate the power unbalance timely, the ESAs should be activated. Meanwhile, this operation can provide enough time for DGAs to compensate power unbalance. To be specific, in this paper, it is assumed that the DGs have enough power to provide for the load, thus the ESAs are used temporarily. The detail algorithm about how to operate ESAs is not discussed in this paper.

Step 3) SDGAs can communicate with its neighbors' information by multi-agent communication protocol which is designed according to the multi-agent consensus algorithm. The deviations of angles and amplitudes of voltages between DGs are calculated by each SDGA through multi-agent consensus algorithm as shown in equation (20) and (21). Then, the deviation should be multiplied with the coupling gains c_1, c_2 and feedback control gains k_1, k_2 as the auxiliary variables shown in equation (25) as the control input into PDGAs.

Step 4) PDGAs need only local information without communication. Each PDGA should establish the nonlinear model of each DG as shown in Section III. Through the feedback linearization method, the nonlinear model can be transformed to the linear model as shown in Section IV-B. This information is embedded in each PDGA which is used to control the local DG. Then, by using the information sent from the SDGAs, the PDGAs can calculate the local control signal according to the equation (43). Finally, the amplitudes and angles of voltages can be synchronized with the leader's information thus the circulating current can be effectively minimized and the output power of DGs can be shared in proportion according to the equation (7) and (8) and the power unbalance can be compensated effectively.

It should be emphasized that not every DGA needs to receive the leader's information because if one DGA can receive the leader information, the other DGAs can produce the reasonable control signal to its own DGs. Thus, Energy Internet can be highly efficient and reliable.

III. THE ANALYSIS OF CIRCULATING CURRENT AND DESIGN OF THE PDGA BASED ON NONLINEAR MODEL OF DG

The control loop, including the power calculation, voltage and current controllers, second order generalized integrator, droop control, is used to achieve local control about the amplitude and angle of output voltage produced by different DGs.

A. Circulating current analysis

Through the circulating current analysis between DGs in [7] the circulating current between two parallel connected DG is divided into active circulating and reactive circulating current as

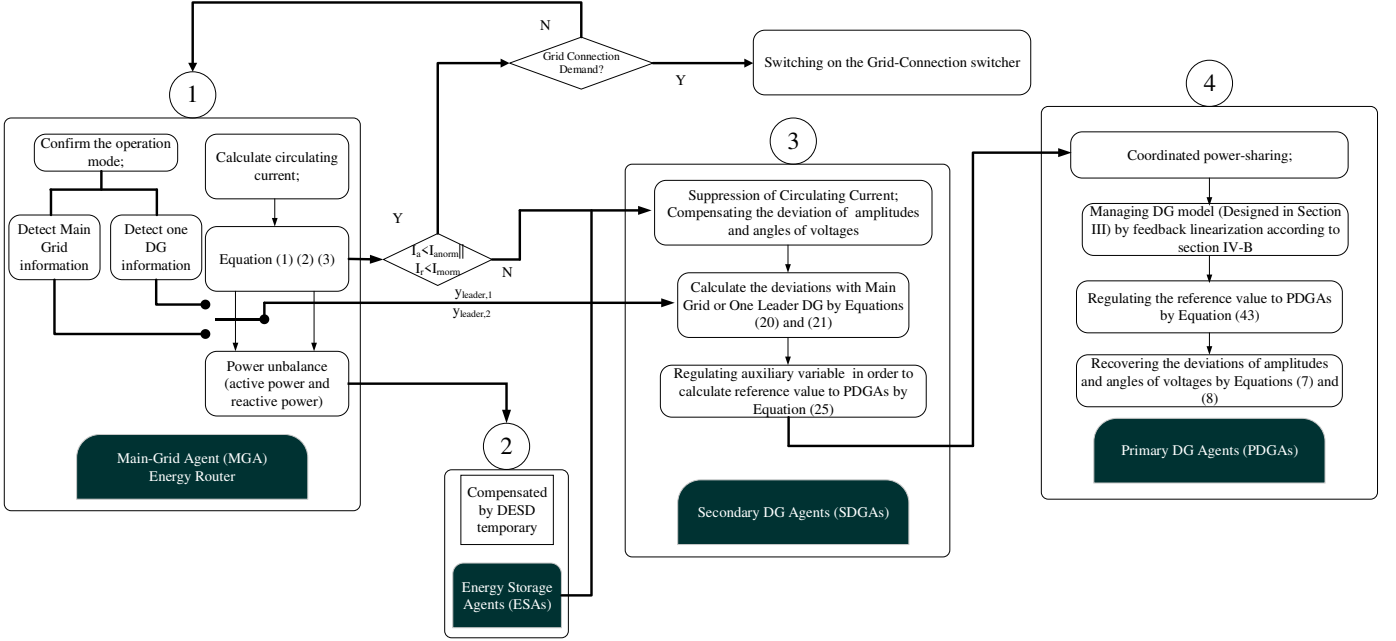$$2\Delta \dot{I} = I_a - jI_r \qquad (1)$$

Fig. 6. Flowchart of the proposed controller for Energy Internet based on Multi-Agent System

$$I_a = \frac{X_k^2 + 4R_o^2}{R_o}\left(E_1' \sin\phi_1 - E_2' \sin\phi_2\right)\frac{1}{A} \qquad (2)$$

$$I_r = \frac{X_k^2 + 4R_o^2}{R_o}\left(E_1' \cos\phi_1 - E_2' \cos\phi_2\right)\frac{1}{A} \qquad (3)$$

where E_1 is output voltage of the first DG, E_2 is output voltage of the second DG, X_{k1}, X_{k2} are line parameters between two DGs, R_o is the load between two DGs, $E_1' = \frac{X_{k2}}{R_o}E_1, E_2' = \frac{X_{k1}}{R_o}E_2$, $A = \left(X_{k1} + X_{k2}\right)^2 + \left(X_{k1}X_{k2}/R_o\right)^2$.

From equations (2) and (3), it can be found that active and reactive circulating currents cannot be effectively eliminated only by controlling the amplitudes or phase angles of the output voltages. Thus the $P-\delta$ and $Q-V$ droops are used to control output voltages amplitudes and angles. In order to mimic the behavior of a synchronous generator, the $P-\delta$ droop control represents the linear relationships between active power and angle of output voltage and the $Q-V$ droop control represents the linear relationships between reactive power and amplitude of output voltage.

B. The design of PDGA combined with nonlinear DG model

In this paper, dc-bus dynamics can be safely neglected, since a dc-link feed forward loop can be used [32]. The block diagram of a DG based on a single-phase inverter is presented in Fig. 7.

The nonlinear dynamics of DGs are controlled under d-q reference frame. In order to mimic a synchronous generator, the d-axis represents direction of rotor magnetic flux linkage and the q-axis is of 90 degrees ahead of d-axis. Thus d-q reference usually forms a rotating orthogonal reference frame used by three-phase DG. However, in this paper single-phase inverters are considered, so that the inverters output voltage and current should be divided first into α-β components

through a second order generalized integrator, as shown in Fig. 8 [33]. To be more specific, the α-β components are the transition reference frame from single-phase reference frame to the d-q reference frame.
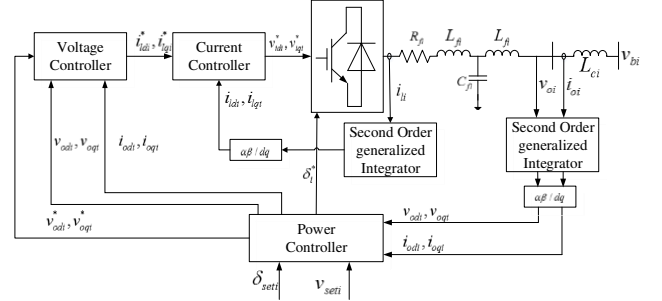
Fig. 7. Block diagram of a DG based on a single-phase inverter

The phase of output voltage of one DG δ_i can be expressed as

$$\dot{\delta}_i = \omega_i \qquad (4)$$
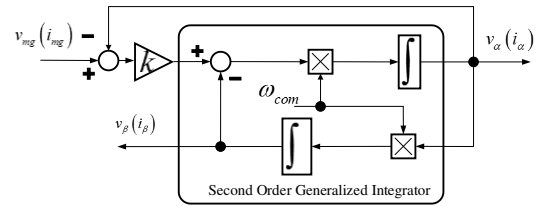
Fig. 8. Second Order Generalized Integrator

Because the $P-\delta$ droop control is used in the system, no frequency deviations would occur under load disturbances.

The power controller shown in Fig. 9 consists of the second order generalized integrator, park transformation, phase-locked loop (PLL), power calculation, low-pass filter and droop controller. The power controller can provide the amplitude reference of voltage v_{odi}^* for the first stage bridge and the angle reference of output voltage δ_i^* for the second

stage bridge. The differential equations of the active and reactive power can be expressed as

$$\dot{P}_i = -\omega_{ci}P_i + \omega_{ci}\frac{\left(v_{odi}i_{odi} + v_{oqi}i_{oqi}\right)}{2} \tag{5}$$

$$\dot{Q}_i = -\omega_{ci}Q_i + \omega_{ci}\frac{\left(v_{odi}i_{oqi} - v_{oqi}i_{odi}\right)}{2} \tag{6}$$

Fig. 9. The block diagram of power controller

The $P-\delta$ and $Q-V$ droop controls are presented as

$$\delta_i^* = \delta_{seti} - m_iP_i \tag{7}$$

$$v_{odi}^* = v_{seti} - n_iQ_i \tag{8}$$

$$v_{oqi}^* = 0 \tag{9}$$

By inserting the (7) and (8) into the (5) and (6), it yields to
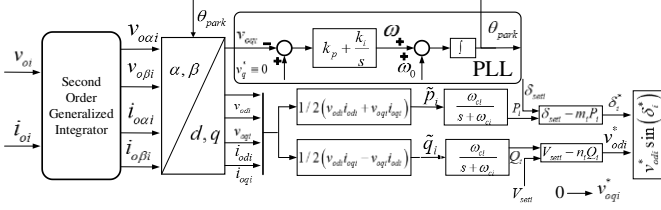
$$\dot{P}_i = \frac{\omega_{ci}}{m_i}\left(\delta_i^* - \delta_{seti}\right) + \omega_{ci}\frac{\left(v_{odi}i_{odi} + v_{oqi}i_{oqi}\right)}{2} \tag{10}$$

$$\dot{Q}_i = \frac{\omega_{ci}}{n_i}\left(v_{odi}^* - v_{seti}\right) + \omega_{ci}\frac{\left(v_{odi}i_{oqi} - v_{oqi}i_{odi}\right)}{2} \tag{11}$$

During the process of our model, the normal control about voltage and current should be included according to [34], as shown in Appendix A.

From the above equations (4) and (10)-(11), and the equations (27), (30)-(32), and (35)-(40) shown in Appendix A, the model of i-th DG can be rewritten into a matrix formation as

$$\begin{cases} \dot{x} = F(x) + gu \\ \quad y = hx \end{cases} \tag{12}$$

where the state vector is
$$x = \left[\delta_i, P_i, Q_i, \phi_{di}, \phi_{qi}, \gamma_{di}, \gamma_{qi}, i_{ldi}, i_{lqi}, v_{odi}, v_{oqi}, i_{odi}, i_{oqi}\right]$$

In order to keep the angle δ_i and the amplitude v_{oi} of the i-th DG being synchronized with other DGs, the δ_{seti} and v_{seti} are selected to be the control inputs. Since v_{oqi} is kept to be zero, the amplitude of output voltage is

$$v_{oi} = v_{odi} \tag{13}$$

Therefore, the inputs of the system are $u = \begin{bmatrix} \delta_{seti} & v_{seti} \end{bmatrix}^T$ and the outputs of the system are $y = \begin{bmatrix} \delta_i & v_{odi} \end{bmatrix}^T$. In the next Section, the feedback linearization method combined with the multi-agent consensus algorithm is used to design the SDGAs.

IV. THE DESIGN OF THE SDGA BASED ON MULTI-AGENT CONSENSUS ALGORITHM

In this Section, the design of the SDGA based on the multi-agent consensus algorithm is proposed by using feedback linearization, which can transform the nonlinear model to the linear model. Each SDGA has two control inputs and two outputs. The consensus problem about angles and amplitudes of output voltages among DGs is the synchronization tracking

problem, which needs a leader in the system. The leader information is decided by the Energy Router. Each SDGA only requires local and its neighbors' information, which can be used to produce the control decision signal. To be more specific, if the leader information in the Energy Router comes from Main-Grid, the Energy Internet can be operated under spinning reserve condition, which means it can be connected to Main-Grid and immediately provide power if necessary.

A. Graph Theory

The distributed coordinated controller should use a communication network called directed graph, which can be expressed as $G_r = \left(V_G, E_G, A_G\right)$ [35]. The set of nodes in the network can be expressed as $V_G = \{v_1, v_2, \cdots v_n\}$, the set of edges can be expressed as $E_G \subseteq V_G \times V_G$ and the weighted adjacency matrix can be expressed as $A_G = \begin{bmatrix} a_{ij} \end{bmatrix}_{n \times n}$ with nonnegative adjacency element a_{ij}. An edge rooted at node j and ended at node i is denoted by $\left(v_j, v_i\right)$, which means that information can flow from the node j to node i. For a graph with 0-1 adjacency elements, the in-degree and out-degree of node v_i are defined as follows:

$$\deg_{in}(v_i) = \sum_{j=1}^{n}a_{ji} \quad \deg_{out}(v_i) = \sum_{j=1}^{n}a_{ij} \tag{14}$$

The degree matrix of diagraph G_r is a diagonal matrix $\Delta = \begin{bmatrix} \Delta_{ij} \end{bmatrix}$ where $\Delta_{ij} = 0$ for all $i \neq j$ and $\Delta_{ii} = \deg_{out}(v_i)$. The Laplacian matrix associated with the digraph G_r is defined as

$$L(G_r) = \Delta - A \tag{15}$$

B. The designation of SDGA

From the discussion in Section III-B, the δ_{seti} is used as the input to control angles of output voltages among different DGs to track the leader $y_{leader,1}$ and the v_{seti} is used as the input to control the amplitude of output voltage to track the voltage $y_{leader,2}$.

The feedback linearization method can establish the relationship between the control outputs and inputs. For the sake of space, the feedback linearization procedures are shown in Appendix B according to [36].

According to process in Appendix B, the relative degree should be calculated first. The relative degree of the nonlinear system is $[1,1]$. The decoupling matrix is calculated as

$$A_i(x) = \begin{pmatrix} \omega_{ci}\delta_{seti} & 0 \\ 0 & \omega_{ci}V_{seti} \end{pmatrix} \tag{16}$$

The matrix $A_i(x)$ is nonsingular. The matrix $b_i(x)$ is calculated as

$$b_i(x) = \begin{bmatrix} L_fh_1(x) & L_fh_2(x) \end{bmatrix}^T \tag{17}$$

where $L_fh_1(x) = \omega_i + \omega_{ci}\left(\delta_{seti} - \delta_i^*\right) - m_i\omega_{ci}\frac{\left(v_{odi}i_{odi} + v_{oqi}i_{oqi}\right)}{2}$

$L_fh_2(x) = \omega_{ci}\left(v_{seti} - v_{odi}^*\right) + n_i\omega_{ci}\frac{\left(v_{odi}i_{oqi} - v_{oqi}i_{odi}\right)}{2} + \omega_iv_{oqi} + \frac{1}{C_{fi}}\left(i_{ldi} - i_{odi}\right)$

From (16) and (17), the control law $u_i(x)$ can be calculated as in (43) (see Appendix B). The $v_i(x)$ can be calculated as follows to achieve the synchronization of y_i.

$$v_i(x) = A_i(x)u_i(x) + b_i(x) \qquad (18)$$

where $v_i = \begin{bmatrix} v_{i,1} & v_{i,2} \end{bmatrix}^T$.

The nonlinear system can be transformed into the following linear system

$$\begin{pmatrix} \dot{y}_{i,1} \\ \dot{y}_{i,2} \end{pmatrix} = \begin{pmatrix} 1 & 0 \\ 0 & 1 \end{pmatrix}\begin{pmatrix} v_{i,1} \\ v_{i,2} \end{pmatrix} \qquad (19)$$

where $y_i = \begin{bmatrix} y_{i,1} & y_{i,2} \end{bmatrix}^T$, $y_{i,1} = \delta_i$, $y_{i,2} = v_{odi}$, $\forall i$, $B = \begin{pmatrix} 1 & 0 \\ 0 & 1 \end{pmatrix}$.

The nonlinear system (12) is transformed to the linear system (19) by using the well-known feedback linearization method. Note that (19) presents the i-th DG linear dynamics.

The control of angles of output voltage is the tracking synchronization problem with a leader in the system. The aim is to make all the angles be equal to the leader. The tracking error is given by

$$e_{i,1} = \sum_{j \in N_i} a_{ij}(y_{i,1} - y_{j,1}) + \varepsilon_{i,1}(y_{i,1} - y_{leader,1}) \qquad (20)$$

where a_{ij} is the element of adjacency matrix, $e_{i,1}$ represents the error of angles of output voltage about the i-th DG. If the node i can receive the leader's angle information, and edge $(v_{leader,1}, v_i)$ is said to exist with weighting gain $\varepsilon_{i,1}$. The node i with $\varepsilon_{i,1} = 1$ is used as a pinned and controlled node about angle. The $\varepsilon_{i,1}$ can be written into matrix as $E_1 = diag\{\varepsilon_{i,1}\} \in R^{N \times N}$.

The control of amplitude of the output voltage is also the tracking synchronization problem with the system leader. Thus, the tracking error is given as

$$e_{i,2} = \sum_{j \in N_i} a_{ij}(y_{i,2} - y_{j,2}) + \varepsilon_{i,2}(y_{i,2} - y_{leader,2}) \qquad (21)$$

where $e_{i,2}$ represents the error of amplitudes of output voltage about the i-th DG. If the node i can receive the leader's amplitude information, and edge $(v_{leader,2}, v_i)$ is said to exist with weighting gain $\varepsilon_{i,2}$. The node i with $\varepsilon_{i,2} = 1$ is used as a pinned and controlled node about amplitude. The $\varepsilon_{i,2}$ can be written into matrix as $E_2 = diag\{\varepsilon_{i,2}\} \in R^{N \times N}$.

The errors can be rewritten by using matrixes as following

$$e_1 = (L + E_1)(Y_1 - Y_{leader,1}) \qquad (22)$$

$$e_2 = (L + E_2)(Y_2 - Y_{leader,2}) \qquad (23)$$

where

$e_1 = \begin{bmatrix} e_{1,1} & e_{2,1} & \cdots & e_{n,1} \end{bmatrix}^T$, $e_2 = \begin{bmatrix} e_{1,2} & e_{2,2} & \cdots & e_{n,2} \end{bmatrix}^T$,

$Y_1 = \begin{bmatrix} y_{1,1} & y_{2,1} & \cdots & y_{n,1} \end{bmatrix}^T$, $Y_{leader,1} = 1_N y_{leader,1}$

$Y_2 = \begin{bmatrix} y_{1,2} & y_{2,2} & \cdots & y_{n,2} \end{bmatrix}^T$, $Y_{leader,2} = 1_N y_{leader,2}$

The system (19) can be rewritten as

$$\begin{cases} \dot{Y}_1 = I_N v_1 \\ \dot{Y}_2 = I_N v_2 \end{cases} \qquad (24)$$

where $v_1 = \begin{bmatrix} v_{1,1} & v_{2,1} & \cdots & v_{n,1} \end{bmatrix}^T$ $v_2 = \begin{bmatrix} v_{1,2} & v_{2,2} & \cdots & v_{n,2} \end{bmatrix}^T$.

The relationship between e_1, e_2 and v_1, v_2 should be designed in order to keep the system stable with the control input.

Let the auxiliary control $v_{i,1}$ and $v_{i,2}$ be defined as follows

$$\begin{cases} v_{i,1} = -c_1 k_1 e_{i,1} \\ v_{i,2} = -c_2 k_2 e_{i,2} \end{cases} \qquad (25)$$

where $c_1, c_2 \in R$ is the coupling gain and $k_1, k_2 \in R$ is the feedback control gain. For sake of space, the detailed design process is not included in this paper.

Remark 1: According to the IEEE 1547-2003 [37], if the amplitudes and angles of output voltages can be kept tracking with the Main-Grid, the system can be connected with Main-Grid if necessary and provide power, which is called spinning reserved condition. Under this condition, the system can compensate the power unbalance with the help from Main-Grid and can also provide the surplus power for Main-Grid. Along with the novel distributed coordinated controller (22)-(25), Energy Internet can be integrated into the Main-Grid seamlessly to provide reserve services at any time to ensure the reliability of the power system as long as the leader information comes from Main-Grid. To be specific, from the perspective of power management, the bidirectional power flow between Main-Grid and Energy Internet can be achieved to compensate power unbalance in both sides. Then Energy Internet can be operated under spinning reserve condition. From the perspective of control method, the angle and amplitude deviations between Main-Grid and Energy Internet are within a small range all the time, thus Energy Internet can be connected to the Main-Grid at any time. Furthermore, various methods on the optimization of spinning reserve condition have also been investigated in [38], [39] and [40], which is out the scope of this paper.

Remark 2: Microgrids and virtual power plants (VPPs) are two recently proposed concepts. Even though lots of control methods for microgrid have been studied, the framework that may encompass a large number of control methods is not completed yet. It means each new control method needs a new control architecture. Meanwhile, VPPs are used to introduce to energy and CO_2-reduction markets more aggressively [41], in which various power production units can cooperate and behave as a single aggregated unit. The power market in microgrids is introduced by the conception of VPPs [42]. Compared with the above two conceptions, the control architecture of Energy Internet including energy router, energy switcher is proposed based on multi-agent system. Meanwhile, the algorithms applied in each agent are studied in this paper.

V. SIMULATION RESULTS

In order to test the proposed approach, a number of simulations under different scenarios have been performed through MATLAB/SIMULINK. The electrical part of the simulation is established through the SIMULINK, meanwhile the control method including the feedback linearization and multi-agent consensus algorithm is programmed through the S-function. Different configurations of loads and DGs are

considered in this section. Fig. 10 shows the configuration of the Energy Internet test system. In addition, the communication structure between agents is also shown in Fig. 10 by dotted lines. In the system, the DG-1 and DG-2 are connected in series and the DG-3 and DG-4 are connected in parallel. This configuration consists of series and parallel connected DGs, which are common in Energy Internet, thus the simulation results can be more convincing. The system data used for simulation are listed in Table I in Appendix C. The numerical values of simulation results are shown in Tables II and III in Appendix C.
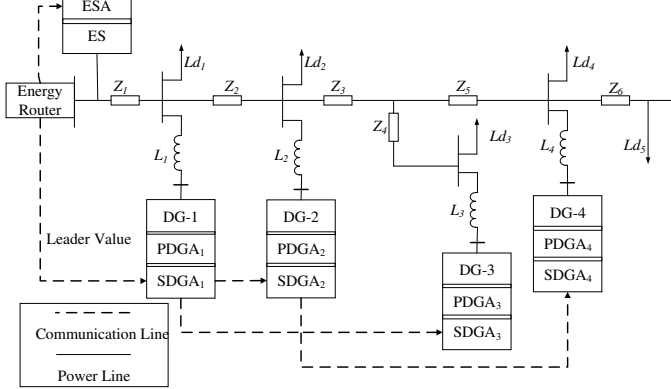

Fig. 10. Configuration of the Energy Internet Test System

A. Case 1: Conventional Controller

In this case, the desired active and reactive ratio of DG-1, DG-2, DG-3 and DG-4 is 1:2:1.33:1.33. To investigate the load sharing with reduced system, DG-4 is disconnected at 0.4s and the load power is shared by DG-1, DG-2 and DG-3. At 0.7s, load-4 and load-5 are also disconnected. The three DGs connected to the Energy Internet supply the 30 kW and 28 kVAr load.
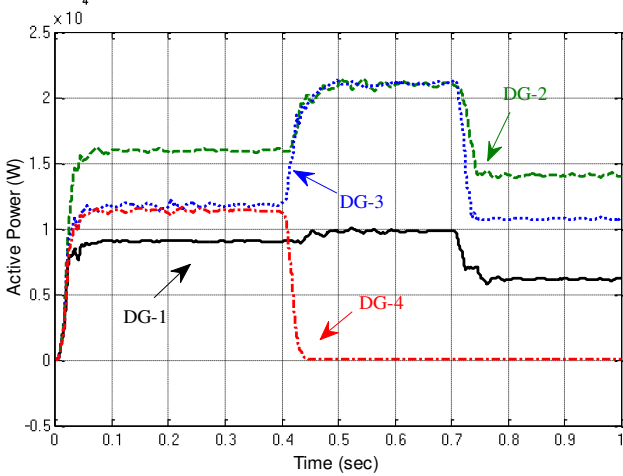

Fig. 11. Active Power-Sharing in Case 1

It can be seen that the system operation is stable. As shown in Figs. 11 and 12, the DGs cannot share loads in the desired ratio of 1:2:1.33. The numerical results can be seen in Table II in Appendix C. In Table II, the output active power and reactive power from four DGs are shown in numerical results and the ratio between each DG output power to DG-1 output power are also shown in Table II. The ratios in "()" are desired ratios between each DG to DG-1. From the numerical results,

it can be found that the output power from four DGs are not according to the desired ratios.

Fig. 12. Reactive Power Sharing in Case 1
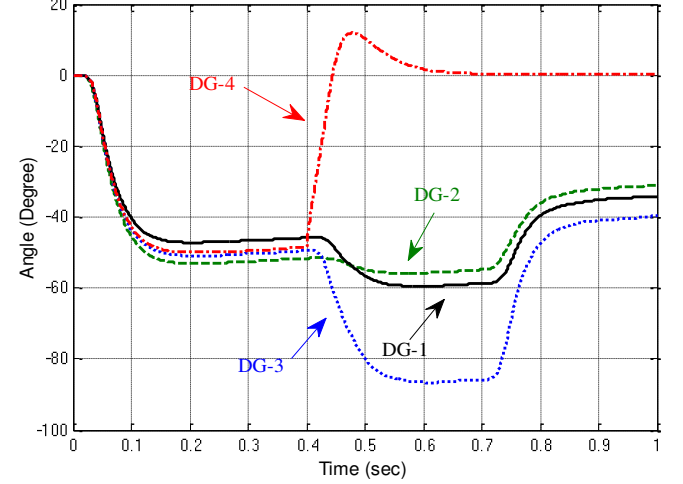
Fig. 13. Angles of Output Voltages from 4 DGs in Case 1
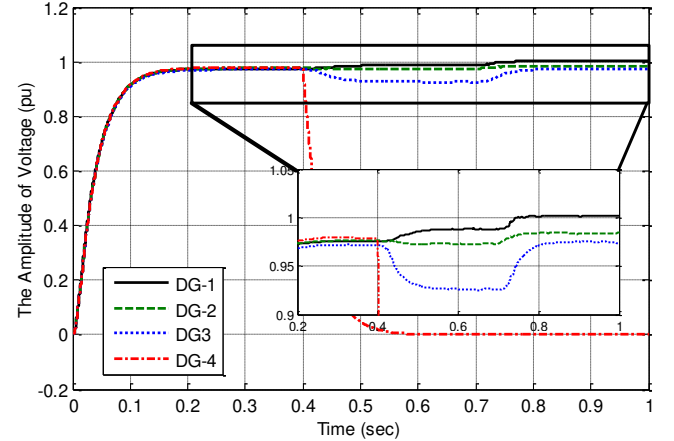
Fig. 14. The p.u. value of Output Voltages from 4 DGs in Case 1

From Figs 13 and 14, the deviations of output voltages from different DGs are large. For one thing, from Fig. 13, at the beginning of the simulation, the angle deviations among four DGs output voltages exist. After 0.4s, the deviations are becoming larger. For another thing, from Fig. 14, after 0.4s, the amplitude deviations between the output voltages are

becoming larger. Thus the conventional control method cannot be effective to control the Energy Internet.

From the above discussion, the deviation angles among the four output currents shown in Fig. 15 are large. According to the equation (1)-(3), the circulating currents between DGs exist very largely in the system. Thus with big deviations between output voltages, if the Energy Internet need to be connected to the Main-Grid, another synchronization algorithm should be added to control the Energy Internet. Thus through the conventional method, the Energy Internet cannot be operated under the spinning reserve condition. And the big circulating currents in Energy Internet can cause unreliability and low power efficiency of the whole system.

Fig. 15. The Output Current in Case 1

B. Case 2: Proposed Controller

To validate the performance of the proposed controller, the Energy Internet is operated at similar situation as described in Case 1.
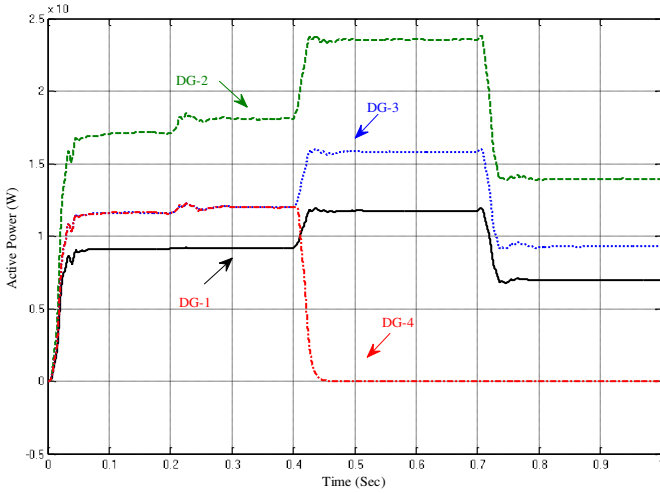
Fig. 16. Active Power Sharing in Case 2

The proposed controller is started at 0.2s. From the communication structure, only DG-1's SDGA can receive the Main-Grid information from the Energy Router. The leader's information is shown in Table. I, Appendix C. The numerical values of power can be seen in Table III, Appendix C. In Table III, the output active power and reactive power from

four DGs are shown in numerical results and the ratio between each DG output power to DG-1 output power are also shown in Table III. The ratios in "()" are desired ratios between each DG to DG-1. Compared with the numerical results in Table II, it can be found that the output power-sharing ratios from four DGs are same with the desired ratios. The accuracies about power sharing can be verified.
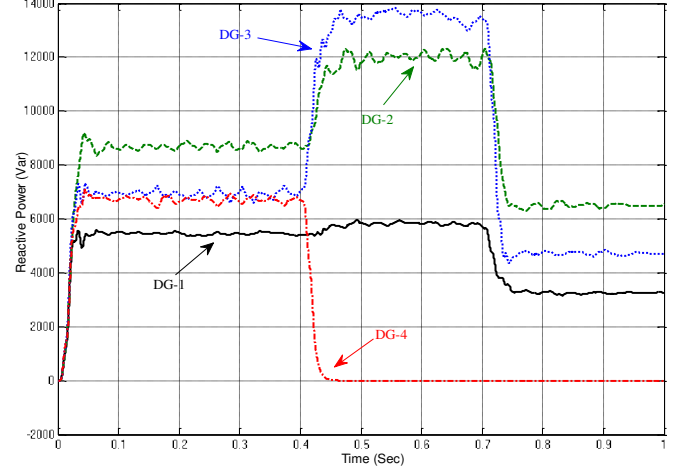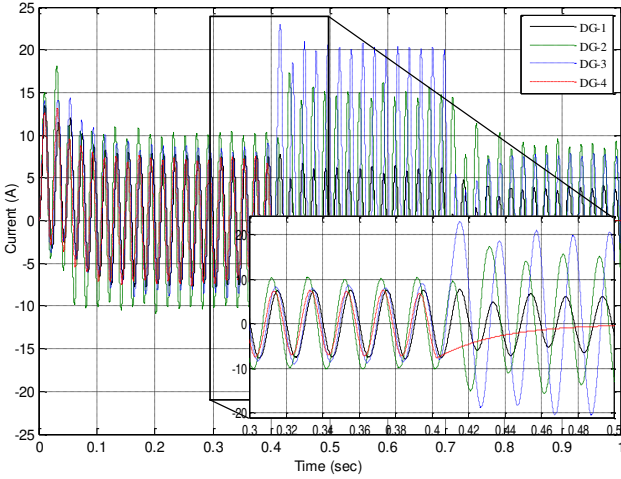

Fig. 17. Reactive Power Sharing in Case 2

Fig. 18. Angles of Output Voltages from 4 DGs in Case 2

Fig. 19. The p.u. value of Output Voltages from 4 DGs in Case 2

Compared with results in Case 1, DGs can share the active power and reactive power in the desired ratio as shown in Figs. 16 and 17. After 0.2s, the amplitudes and angles of output voltages from DGs begin to reach a consensus with the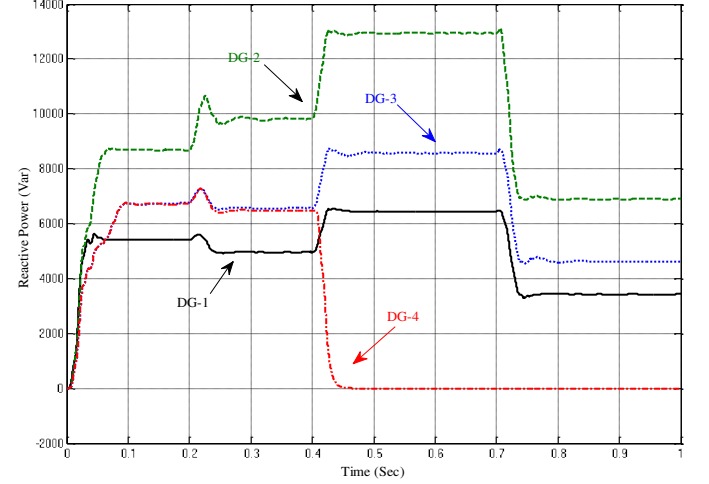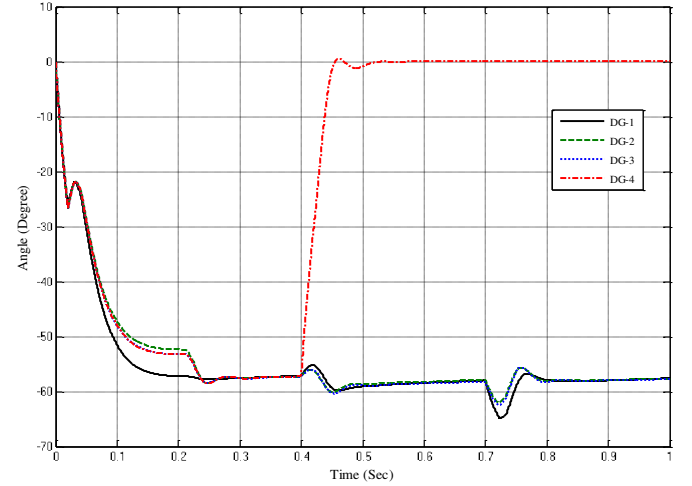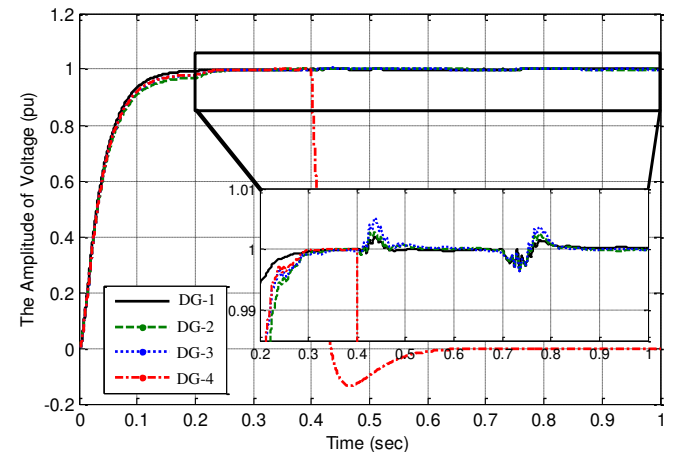 leader shown in Figs. 18 and 19. Thus the amplitude of output currents of four DGs are in desired ratio and the deviation angles between four output currents are very small as shown in Fig. 20. From the equation (2) and (3), the circulating current between DGs can be minimized.

Furthermore, since both angles and amplitudes of DGs output voltages in the Energy Internet can be controlled to reach consensus with the Main-Grid information due to the proposed method. With enough energy storage, the Energy Internet can be operated under spinning reserve condition.
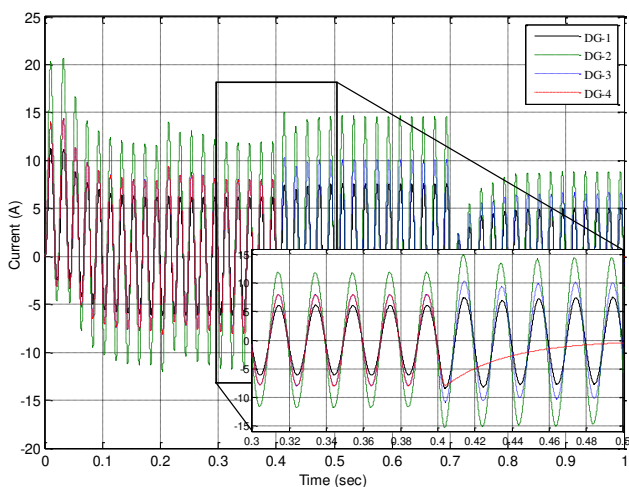

Fig. 20. The Output Current in Case 2

Remark 3: Since large circulating currents in the Energy Internet can cause large unnecessary power losses, to reduce the circulating current can effectively decrease power losses in the Energy Internet.

VI. COMPARISON BETWEEN THE PROPOSED DISTRIBUTED APPROACH WITH THE CENTRALIZED APPROACH

A. Comparison about computational power

When a centralized controller is used, all the system information should be communicated to the central unit. With the increasing number of DGs and other energy sources, the communication burden may increase due to the additional variables and constraints. Meanwhile, the computation time of such a central controller is highly dependent on the number of devices in the control system. Thus large communication delays may occur in the system which may cause serious negative influence on the stability and system performances, thus reducing the system scalability drastically.

By comparison, in proposed controller, there is no centralized controller in the system and the communication load for each controller is uncorrelated with the increasing number of controllers in the system. Since the multi-agent consensus algorithm is applied in this paper, each controller only needs its local information and at least one of its neighbors' information. Thus each controller's computation

load is nearly constant when controllers are added or removed from the control system.

The same results about the comparison of the computational power between distributed controller and centralized controller can be also found in [20].

B. Comparison with the performance, resilience and scalability

When the system does not present faults, the performances between distributed or centralized controllers are almost equal. Indeed the centralized controller gives all the local DGs the same control signal, while the distributed controller make control decision of each DG according to its neighbors information. Thus the response speed of the distributed controller can be faster than that of centralized controller.

Under fault conditions, if the centralized controller fails down, the whole system will lose the control and may become unstable. By comparison, once one distributed controller fails down, it cannot cause serious influence on the whole system. The reason of this is that each controller only needs its local and neighbors' information based on sparse communication structure. Furthermore, if this controller cannot be recovered in a short time, we can disconnect it to maintain the stability of the whole system. However if the centralized controller cannot be recovered timely, it may not be possible to maintain stable operation. The stability about multi-agent consensus algorithm considering switching topology has been proved in several previous works like those in [43] [44]. In the future, this algorithm may be extended to the distributed controllers. Thus resilience of the distributed controller can be much better than the centralized controller one.

Based on the proposed algorithm combined with the multi-agent system, the distributed controller in this paper is still open for improvement, because several conditions are not included in this paper. Section VIII discusses some possibilities of improvement for reference to the interested reader. Meanwhile, the scale of the distributed system can be enlarged without communication limits, computation limits and algorithm limits. By comparison, the scale of the centralized controller is limited by its communication and computation ability. Thus the scalability of distributed controller is much higher than that of centralized controller.

VII. CONCLUSION

The control issues of in Energy Internet were investigated in this paper. The multi-agent consensus algorithm and multi-agent system architecture are combined to design the control structure and control method applied in Energy Internet. The decomposed tasks, established and transformed model, information flow for each agent are studied. The benefits of this paper are as follows: 1) The combination of multi-agent system and multi-agent consensus algorithm will provide an infrastructure for future research used in Energy Internet. 2) The circulating current reduction in Energy Internet and proportional power-sharing to the desired ratio among DGs can be guaranteed by combining with the P-δ and Q-V controllers and multi-agent consensus algorithms. 3) The output voltages in Energy Internet can be recovered while being synchronized with the leader information from Main-

Grid, which means the Energy Internet can operate as spinning reserve system. 4) For daily life, with sparse communication systems and bidirectional power flows, Energy Internet provides customers a reliable and efficient power supply, while minimizing energy costs and providing the different types of renewable energy resources the possibility to plug-in/out at any time.

VIII. FUTURE WORK

Future work will consist of, but will not be limited to, the following aspects:

1). The cost, location elements should be considered when the proposed algorithm decides the power sharing in Energy Internet. In this paper, the power sharing between different DGs only base on their rated power, but in practical the economic element is another important index. Meanwhile, the power market should be studied in Energy Internet in order to make the system operated more economical.

2). The changes of communication topology should be considered in the future. In this paper, the communication topology in the control system is kept constant. In the future, the switching topology multi-agent consensus algorithm should be applied in the control system. With this application, the comparison about resilience between distributed controller and centralized controller could be more obvious.

3). The cost about hardware during the process of designation should be considered in the future. In this paper, the cost about hardware between distributed controller and centralized controller are not compared which can illustrate benefits about distributed controller furthermore.

4). In this paper, we only introduce a little about the energy storage without its control strategy. Because the energy storage is very important under some extremely conditions, the control strategy for energy storage should be studied based on the proposed control architecture in the future.

APPENDIX A

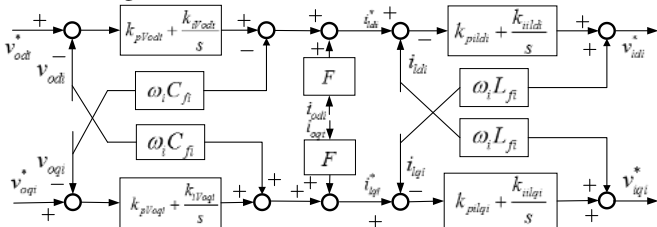The block diagram of the voltage and current controller is shown in Fig. 21.

Fig. 21. The Block diagram of the voltage and current controller

The differential equations of the voltage controller are presented as

$$\dot{\phi}_{odi} = v^*_{odi} - v_{odi} \tag{26}$$

$$\dot{\phi}_{oqi} = v^*_{oqi} - v_{oqi} \tag{27}$$

The outputs of the voltage controller are presented as

$$i^*_{ldi} = F i_{odi} - \omega_f C_f v_{oqi} + k_{pVodi}\left(v^*_{odi} - v_{odi}\right) + k_{iVodi}\phi_{odi} \tag{28}$$

$$i^*_{lqi} = F i_{oqi} - \omega_f C_f v_{odi} + k_{pVoqi}\left(v^*_{oqi} - v_{oqi}\right) + k_{iVoqi}\phi_{oqi} \tag{29}$$

In addition, inserting (8) into (26), we obtain

$$\dot{\phi}_{odi} = v_{seti} - n_i Q_i - v_{odi} \tag{30}$$

The differential equations of the current controller are presented as

$$\dot{\gamma}_{di} = i^*_{ldi} - i_{ldi} \tag{31}$$

$$\dot{\gamma}_{qi} = i^*_{lqi} - i_{lqi} \tag{32}$$

The outputs of the current controller are presented as

$$v^*_{idi} = -\omega_f L_f i_{lqi} + k_{pildi}\left(i^*_{ldi} - i_{ldi}\right) + k_{iildi}\gamma_{di} \tag{33}$$

$$v^*_{iqi} = \omega_f L_f i_{ldi} + k_{pilqi}\left(i^*_{lqi} - i_{lqi}\right) + k_{iilqi}\gamma_{qi} \tag{34}$$

Fig. 2 shows that the connection between inverters are inductive. The differential equations for the output LCL filter L_{fi} and C_{fi} and the output inductor L_{Ci} are expressed as follows.

$$\dot{i}_{ldi} = -\frac{R_{fi}}{L_{fi}} i_{ldi} + \omega_i i_{lqi} + \frac{1}{L_{fi}}\left(v_{idi} - v_{odi}\right) \tag{35}$$

$$\dot{i}_{lqi} = -\frac{R_{fi}}{L_{fi}} i_{lqi} - \omega_i i_{ldi} + \frac{1}{L_{fi}}\left(v_{iqi} - v_{oqi}\right) \tag{36}$$

$$\dot{v}_{odi} = \omega_i v_{oqi} + \frac{1}{C_{fi}}\left(i_{ldi} - i_{odi}\right) \tag{37}$$

$$\dot{v}_{oqi} = -\omega_i v_{odi} + \frac{1}{C_{fi}}\left(i_{lqi} - i_{oqi}\right) \tag{38}$$

$$\dot{i}_{odi} = \omega_i i_{oqi} + \frac{1}{L_{ci}}\left(v_{odi} - v_{bdi}\right) \tag{39}$$

$$\dot{i}_{oqi} = -\omega_i i_{odi} + \frac{1}{L_{ci}}\left(v_{oqi} - v_{bqi}\right) \tag{40}$$

APPENDIX B

The process of establishing the relationship in a MIMO nonlinear system described in (12) is explained below.

First, the relative degree $[r_1, r_2, \cdots, r_m]$ should be calculated.

Second, according to the relative degree, a decoupling matrix $A(x)$ which should be nonsingular should be calculated as given in (41), another vector $b(x)$ should be calculated at the same time as in (42). In (41) and (42), $L_f h_i(x)$ is the Lie derivative of $h_i(x)$ with respect to f and is defined as $L_f h_i(x) = \left(\partial(h_i)/\partial x_i\right)f$.

$$A(x) = \begin{pmatrix} L_{g_1} L_f^{r_1-1} h_1(x) & \cdots & L_{g_m} L_f^{r_1-1} h_1(x) \\ \vdots & & \vdots \\ L_{g_1} L_f^{r_1-1} h_m(x) & \cdots & L_{g_m} L_f^{r_1-1} h_m(x) \end{pmatrix} \tag{41}$$

$$b(x) = \left[L_f^{r_1} h_1(x) \cdots L_f^{r_m} h_m(x)\right]^T \tag{42}$$

Third, based on the defined relative degree, the control law of a MIMO nonlinear system is defined as

$$u(x) = A^{-1}(x)\left[-b(x) + v(x)\right] \tag{43}$$

where $v(x) = \left[v_1 \cdots v_m\right]^T = \left[y_1^{(r_1)} \cdots y_m^{(r_m)}\right]^T$.

Appendix C
TABLE I
SYSTEM PARAMETERS

System Quantities	Values
System Frequency	50Hz
DC voltage	800V
Leader information Voltage	1p.u

Angle	57.4 degree
Line impedance $Z_1=Z_2=Z_3=Z_4=Z_5=Z_6$	$0.05+j1.5*10^{-5}\Omega$
Load Ratings	
Ld_1	10.1 KW and 5 kVAr
Ld_2	10.1 KW and 5 kVAr
Ld_3	10.1 KW and 5 kVAr
Ld_4	10 KW and 6 kVAr
Ld_5	11 KW and 7 kVAr
DG ratings	
DG-1	10 KW and 5 kVAr
DG-2	20 KW and 10 kVAr
DG-3	13.3 KW and 6.6 kVAr
DG-4	13.3 KW and 6.6 kVAr
Output inductances	
L_1	10 µH
L_2	5 µH
L_3	7.51 µH
L_4	7.51 µH
Droop Coefficients Active Power-Angle	
m_1	$1*10^{-4}$ rad/w
m_2	$5*10^{-5}$ rad/w
m_3	$7.5*10^{-5}$ rad/w
m_4	$7.5*10^{-5}$ rad/w
Reactive Power-Voltage	
n_1	$4*10^{-4}$ rad/VAr
n_2	$2*10^{-4}$ rad/VAr
n_3	$3*10^{-4}$ rad/VAr
n_4	$3*10^{-4}$ rad/VAr

TABLE II
NUMERICAL RESULTS OF CASE I

CASE-1: Section V. A Reduced System of Fig. 7 without Proposed Controller			
Active Power	Initial Value (0s-0.4s)	Intermediate Value (0.4s-0.7s)	Final Value (0.7s-1s)
P_{DG-1}	9.1 kW	9.8 kW	6 kW
P_{DG-2}	17.1 kW	21 kW	14kW
P_{DG-3}	11.6 kW	21 kW	11kW
P_{DG-3}	11.6 kW	0 kW	0kW
Active Power Ratio of P_{DG-1}	Initial Value (0s-0.4s)	Intermediate Value (0.4s-0.7s)	Final Value (0.7s-1s)
P_{DG-1}	1.0 (1.0)	1.0 (1.0)	1.0 (1.0)
P_{DG-2}	1.879 (2.0)	2.143 (2.0)	2.333 (2.0)
P_{DG-3}	1.26 (1.33)	2.142(1.33)	1.83 (1.33)
P_{DG-4}	1.26 (1.33)	0.0 (0.0)	0.0 (0.0)
Reactive Power	Initial Value (0s-0.4s)	Intermediate Value (0.4s-0.7s)	Final Value (0.7s-1s)
P_{DG-1}	5.4 kVAr	5.8 kVAr	3.2kVAr
P_{DG-2}	8.7 kVAr	12 kVAr	6.1kVAr
P_{DG-3}	6.8 kVAr	13 kVAr	4.7 kVAr
P_{DG-3}	6.9 kVAr	0 kVAr	0 kVAr
Reactive Power Ratio of P_{DG-1}	Initial Value (0s-0.4s)	Intermediate Value (0.4s-0.7s)	Final Value (0.7s-1s)
P_{DG-1}	1.0 (1.0)	1.0 (1.0)	1.0 (1.0)
P_{DG-2}	1.61 (2.0)	2.06 (2.0)	1.9 (2.0)
P_{DG-3}	1.29 (1.33)	2.24 (1.33)	1.469 (1.33)
P_{DG-4}	1.27 (1.33)	0.0 (0.0)	0.0 (0.0)

TABLE III
NUMERICAL RESULTS OF CASE II

CASE-2: Section V. B Reduced System with Proposed Controller				
Active Power	Initial Value (0s-0.2s)	Intermediate Value 1 (0.2s-0.4s)	Intermediate Value 2 (0.4s-0.7s)	Final Value (0.7s-1s)
P_{DG-1}	9.1 kW	9.2 kW	11.7 kW	7.0 kW
P_{DG-2}	17.1 kW	18.2 kW	23.6 kW	13.9 kW
P_{DG-3}	11.6 kW	12 kW	15.7 kW	9.3 kW
P_{DG-4}	11.6 kW	12 kW	0 kW	0 kW
Active Power Ratio of P_{DG-1}	Initial Value (0s-0.2s)	Intermediate Value 1 (0.2s-0.4s)	Intermediate Value 2 (0.4s-0.7s)	Final Value (0.7s-1s)
P_{DG-1}	1.0 (1.0)	1.0 (1.0)	1.0 (1.0)	1.0 (1.0)
P_{DG-2}	1.879 (2.0)	1.978 (2.0)	2.017 (2.0)	1.986 (2.0)
P_{DG-3}	1.26 (1.33)	1.304 (1.33)	1.341 (1.33)	1.328 (1.33)
P_{DG-4}	1.26 (1.33)	1.304 (1.33)	0.0 (0.0)	0.0 (0.0)
Reactive Power	Initial Value (0s-0.2s)	Intermediate Value 1 (0.2s-0.4s)	Intermediate Value 2 (0.4s-0.7s)	Final Value (0.7s-1s)
P_{DG-1}	5.4 kVAr	4.9 kVAr	6.45 kVAr	3.5 kVAr
P_{DG-2}	8.7 kVAr	9.9 kVAr	12.95kVAr	6.87 kVAr
P_{DG-3}	6.8 kVAr	6.6 kVAr	8.55 kVAr	4.63 kVAr
P_{DG-4}	6.7 kVAr	6.5 kVAr	0 kVAr	0 kVAr
Reactive Power Ratio of P_{DG-1}	Initial Value (0s-0.2s)	Intermediate Value 1 (0.2s-0.4s)	Intermediate Value 2 (0.4s-0.7s)	Final Value (0.7s-1s)
P_{DG-1}	1.0 (1.0)	1.0 (1.0)	1.0 (1.0)	1.0 (1.0)
P_{DG-2}	1.61 (2.0)	2.02 (2.0)	2.01 (2.0)	1.96 (2.0)
P_{DG-3}	1.26 (1.33)	1.34 (1.33)	1.33 (1.33)	1.32 (1.33)
P_{DG-4}	1.24 (1.33)	1.33 (1.33)	0.0 (0.0)	0.0 (0.0)

IX. REFERENCES

[1] A. Q. Huang, M. L. Crow, G. T. Heydt, J. P. Zheng, and S. J. Dale, "The future renewable electric energy delivery and management system: The energy internet," in *Proc. IEEE*, vol. 99, no. 1, pp. 133-148, Jan. 2011.

[2] X. Yu, X. She, X. Ni, and A. Q. Huang, "System integration and hierarchical power management strategy for a solid-state transformer interfaced microgrid system," *IEEE Trans. Power Electron.*, vol. 29, no. 8, pp. 4414-4425, Aug. 2014.

[3] X. Yu, X. She, X. Zhou, and A. Q. Huang, "Power management for dc microgrid enabled by solid-state transformer," *IEEE Trans. Smart Grid*, vol. 5, no. 2, pp. 954-965, Mar. 2014.

[4] M. C. Chandorkar, D. M. Divan, R. Adapa, "Control of parallel connected inverters in standalone ac supply systems," *IEEE Trans. Ind. Appl.*, vol. 29, no. 1, pp. 136-143, Jan/Feb. 1993.

[5] Q. Sun, J. Zhou, J. M. Guerrero, and H. Zhang, "Hybrid three-phase/single-phase microgrid architecture with power management capabilities," *IEEE Trans. Power Electron.*, Published on-line, 2014, DOI: 10.1109/TPEL.2014.2379925

[6] S. V. Iyer, M. N. Belur, and M. C. Chandorkar, "Analysis and mitigation of voltage offsets in multi-inverter microgrids," *IEEE Trans. Energy Convers.*, vol. 26, no. 1, pp. 354-363, Mar. 2011.

[7] Z. Ye, P. K. Jain, P. C. Sen, "Circulating current minimization in high–frequency AC power distribution architecture with multiple inverter modules operated in parallel," *IEEE Trans Ind. Electron.*, vol. 54, no. 5, pp. 2673-2687. Oct. 2007.

[8] J. M. Guerrero, J. C. Vasquez, J. Matas, J. G. de Vicuna, and M. Castilla, " Hierarchical control of droop-controlled AC and DC microgrids—a general approach toward standardization." *IEEE Trans Ind. Electron.*, vol. 58, no. 1, pp. 158-172. Jan. 2011.

[9] Y. W. Li, and C.-N. Kao, "An accurate power control strategy for power-electronics-interfaced distributed generation units operating in a low-voltage multibus microgrid," *IEEE Trans. Power Electron.*, vol. 24, no. 12, pp. 2977-2988, Dec. 2009.

[10] A. Bidram, A. Davoudi, F. L. Lewis, and S. S. Ge, "Distributed adaptive voltage control of inverter-based microgrids," *IEEE Trans. Energy Convers.*, to be published.

[11] J. M. Guerrero, L. Hang, J. Uceda, "Control of distributed uninterruptible power supply systems," *IEEE Trans Ind. Electron.*, vol. 55, no. 8, pp. 2845-2859. Aug. 2008.

[12] X. Lu, J. M. Guerrero, K. Sun, J. C. Vasquez, R. Teodorescu, and L. Huang, "Hierarchical control of parallel ac-dc converter interfaces for hybrid microgrids," *IEEE Trans. Smart Grid*, vol. 5, no. 2, pp. 683-692, Mar. 2014.

[13] M. Savaghebi, A. Jalilian, J. C. Vasquez, and J. M. Guerrero, "Secondary control scheme for voltage unbalance compensation in an islanded droop-controlled microgrid," *IEEE Trans. Smart Grid*, vol. 3, no. 2, pp. 797-807, Mar. 2014.

[14] H. Zhang, T. Feng, G. Yang, and H. Liang, "Distributed cooperative optimal control for multiagent systems on directed graphs: an inverse optimal

approach," *IEEE Trans. Cyber.*, published on-line on 1st, Sep. 2014, DOI: 10.1109/TCYB.2014.2350511.

[15] H. Zhang, J. Zhang, G. Yang, and Y. Luo, " Leader-based optimal coordination control for the consensus problem of multi-agent differential games via fuzzy adaptive dynamic programming," *IEEE Trans. Fuzzy Syst.*, vol. 23, no. 1, pp. 152-163, 2015.

[16] A. L. Dimeas, N. D. Hatziargyriou, "Operation of a multiagent system for microgrid control," *IEEE Trans. Power Syst.*, vol. 20, no. 3, pp. 1447-1455, Aug. 2005.

[17] P. Papadopoulos, N. Jenkins, L. M. Cipcigan, I. Grau, E. Zabala, "Coordination of the charging of electric vehicles using a multi-agent system," *IEEE Trans. Smart Grid*, vol. 4, no. 4, pp. 1802-1809, Dec. 2013.

[18] E. L. Karfopoulos, N. D. Hatziargyriou, "A multi-agent system for controlled charging of a large population of electric vehicles," *IEEE Trans. Power Syst.*, vol. 28, no. 2, pp. 1196-1204, May 2013.

[19] A. Bidram, A. Davoudi, F. L. Lwis, and J. M. Guerrero, "Distributed cooperative secondary control of microgrids using feedback linearization," *IEEE Trans. Power Syst.*, vol. 28, no. 3, pp. 3462-3470, Aug. 2013.

[20] W. Liu, W. Gu, W. Sheng, X. Meng, Z. Wu, and W. Chen, "Decentralized multi-agent system-based cooperative frequency control for autonomous microgrid with communication constraints," *IEEE Trans. Sustain. Energy*, vol. 5, no. 2, pp. 446-456, Apr. 2014.

[21] W. Yao, M. Chen, J. Matas, J. M. Guerrero, and Z. M. Qian, "Design and analysis of the droop control method for parallel inverters considering the impact of the complex impedance on the power sharing," *IEEE Trans. Ind. Electron.*, vol. 58, no. 2, pp. 576-588, Feb. 2011.

[22] J. E. Slotine and W. Li, *Applied Nonlinear Control*. Upper Saddle River, NJ, USA: Prentice-Hall, 2009.

[23] H. Zhang, D. Liu, Y. Luo, and D. Wang, *Adaptive Dynamic Programming for Control-Algorithms and Stability*. London: Springer-Verlag, 2013.

[24] M. Q. Wang, and H. B. Gooi, "Spinning reserve estimation in microgrids," *IEEE Trans. Power Syst.*, vol. 26, no. 3, pp. 1164-1174, Aug. 2011.

[25] Y. Rebours and D. S. Kirschen, What is Spinning Reserve?, 2005. [Online].
Available:http://eee.dev.ntweb.mcc.ac.uk/research/groups/eeps/publications/reportstheses/aoe/rebours et al_tech rep_2005A.pdf.

[26] L. Rao, X. Liu, M. D. Ilic, and J. Liu, "Distributed coordination of internet data centers under multiregional electricity markets," in *Proc. IEEE*, vol. 100, no. 1, pp. 269-282, Jan. 2012.

[27] T. L. Vandoorn, J. C. Vasquez, J. D. Kooning, J. M. Guerrero, and L. Vandevelde, "Microgrids: hierarchical control and overview of the control and reserve management strategies," *IEEE Ind. Electron. Mag.*, vol. 7, no. 4, pp. 42-55, Dec. 2013.

[28] C. Yuen, A. Oudalov, and A. Timbus, "The provision of frequency control reserves from multiple microgrids," *IEEE Trans. Ind. Electron.*, vol. 58, no. 1, pp. 173–183, Jan. 2011.

[29] E. M. Davidson, S. D. J. McArthur, J. R. McDonald, T. Cumming, I. Watt, "Applying multi-agent system technology in practice: automated management and analysis of SCADA and digital fault recorder data," *IEEE Trans. Power Syst.*, vol. 21, no. 2, pp. 559-567, Aug. 2006.

[30] J. A. Hossack, J. Menal, S. D. J. McArthur, J. R. McDonald, "A multiagent architecture for protection engineering diagnostic assistance," *IEEE Trans. Power Syst.*, vol. 18, no. 2, pp. 639-647, May 2003.

[31] M. Wooldridge, N. R. Jennings, and D. Kinny, "The gaia methodology for agent-oriented analysis and design," *Journal of Autonomous Agents and Multi-Agent Systems*, vol. 3, pp. 285-312, 2000.

[32] J. C. Vasquez, J. M. Guerrero, M. Savaghebi, J. Eloy-Garcia, R. Teodorescu, "Modeling, analysis, and design of stationary-reference-frame droop-controlled parallel three-phase voltage source inverters," *IEEE Trans Ind. Electron.*, vol. 60, no. 4, pp. 1271-1280. Apr. 2013.

[33] M. Ciobotaru, R. Teodorescu, F. Blaabjerg, "A new single-phase PLL structure based on second order generalized integrator," in *Proc. 2006 IEEE Power Electronics Specialists Conf.*, 2006, pp. 1-6.

[34] N. Pogaku, M. Prodanovic, and T. C. Green, "Modeling, analysis and testing of autonomous operation of an inverter-based microgrid," *IEEE Trans. Power Electron.*, vol. 22, no. 2, pp. 613–625, Mar. 2007.

[35] C. Godsil and G. Royle, *Algebraic Graph Theory*. New York: Springer-Verlag, 2001, vol. 207, Graduate Texts in Mathematics.

[36] F. L. Lewis and V. L. Syrmos, *Optimal Control*. New York: USA: Wiley, 1995.

[37] IEEE 1547-2003. Standard for interconnecting distributed resources with electric power system[S]. *American, IEEE committee*, 2003

[38] L.-R. Chang-Chien, L. N. An, T.-W. Lin, and W.-J. Lee, "Incorporating demand response with spinning reserve to realize an adaptive frequency restoration plan for system contingencies," *IEEE Trans. Smart Grid*, vol. 3, no. 3, pp. 1145-1153, Sep. 2012.

[39] A. Ahmadi-Khatir, M. Bozorg, and R. Cherkaoui, "Probabilistic spinning reserve provision model in multi-control zone power system," *IEEE Trans. Power Syst.*, vol. 28, no. 3, pp. 2819-2829, Aug. 2013.

[40] S. Lou, S. Lu, Y. Wu, and D. S. Kirschen, "Optimizing spinning reserve requirement of power system with carbon capture plants," *IEEE Trans. Power Syst.*, vol. pp, no. pp, 1-8, to be published.

[41] A. L. Dimeas, N. D. Hatziargyriou, "Agent based control of Virtual Power Plants," in *Proc. Int. Conf. Intelligent Syst. Applications to Power Syst.* Jan. 2007.

[42] O. Palizban, K. Kauhaniemi, J. M. Guerrero, "Microgrids in active network management-Part I: Hierarchical control, energy storage, virtual power plants, and market participation," *Renewable and Sustainable Energy Reviews*, vol. 36, pp. 428-439, Jan. 2014.

[43] U. Munz, A. Papachristodoulou, F. Allgower, "Consensus in multi-agent systems with coupling delays and switching topology," *IEEE Trans. Autom. Control*, vol. 56, no. 12, pp. 2976-2982, Dec. 2011.

[44] J. Qin, C. Yu, S. Hirche, "Stationary consensus of asynchronous discrete-time second-order multi-agent systems under switching topology," *IEEE Trans. Industrial Informatics*, vol. 8, no. 4, pp. 986-994, Nov. 2012.

Qiuye Sun (M'11−) received the B.S. degree in power system and its automaton from the Northeast Dianli University of China, Jilin City, China, in 2000, the M.S. degree in power electronics and drives, and the Ph.D. degree in control theory and control engineering from the Northeastern University, Shenyang, China, in 2004 and 2007, respectively. Since 2014, he has been a Full Professor with the School of Information Science and Engineering, Northeastern University, China.

His main research interests are optimization and control of smart grid, and network control of distributed generation system, microgrids, and Energy Internet. He has authored and coauthored over 280 journal and conference papers, six monographs and co-invented 90 patents.

Renke Han was born in Anshan, Liaoning Province, China, in 1991. He received the B.S. degree in automation from the Northeastern University, Shenyang, China, in 2013. He is currently working toward the M.S. degree in control theory and control engineering from the Northeastern University, Shenyang, China.

His current research interests include network control, hierarchical and distributed coordinated control, and power flow management strategy in microgrid and Energy Internet.

Huaguang Zhang (M'03−SM'04−F'14) received the B.S. degree and the M.S. degree in control engineering from Northeast Dianli University of China, Jilin City, China, in 1982 and 1985, respectively. He received the Ph.D. degree in thermal power engineering and automation from Southeast University, Nanjing, China, in 1991.

He joined the Department of Automatic Control, Northeastern University, Shenyang, China, in 1992, as a Postdoctoral Fellow for two years. Since 1994, he has been a Professor and Head of the Institute of Electric Automation, School of Information Science and Engineering, Northeastern University, Shenyang, China. His main research interests are fuzzy control, stochastic system control, neural networks based control, nonlinear control, and their applications. He has authored and coauthored over 280 journal and conference papers, six monographs and co-invented 90 patents.

Dr. Zhang is Chair of the Adaptive Dynamic Programming & Reinforcement Learning Technical Committee on IEEE Computational Intelligence Society. He is an Associate Editor of AUTOMATICA, IEEE TRANSACTIONS ON

NEURAL NETWORKS, IEEE TRANSACTIONS ON CYBERNETICS, and NEUROCOMPUTING, respectively. He was an Associate Editor of IEEE TRANSACTIONS ON FUZZY SYSTEMS (2008-2013). He was awarded the Outstanding Youth Science Foundation Award from the National Natural Science Foundation Committee of China in 2003. He was named the Cheung Kong Scholar by the Education Ministry of China in 2005. He is a recipient of the IEEE Transactions on Neural Networks 2012 Outstanding Paper Award.

Jianguo Zhou was born in Yunnan, China, in 1987. He received the B.S. degree in automation, and the M.S. degree in control theory and control engineering from the Northeastern University, Shenyang, China, in 2011 and 2013, respectively. He is currently working toward the Ph.D. degree in control theory and control engineering from the Northeastern University, Shenyang, China.

His current research interests includes power electronics, hierarchical and distributed cooperative control, and power quality improvement of microgrids, and synchronization of complex/multi-agent networks and their applications in microgrids and Energy Internet.

Josep M. Guerrero (S'01-M'04-SM'08-F'14) received the B.S. degree in telecommunications engineering, the M.S. degree in electronics engineering, and the Ph.D. degree in power electronics from the Technical University of Catalonia, Barcelona, in 1997, 2000 and 2003, respectively. Since 2011, he has been a Full Professor with the Department of Energy Technology, Aalborg University, Denmark, where he is responsible for the Microgrid Research Program. From 2012 he is a guest Professor at the Chinese Academy of Science and the Nanjing University of Aeronautics and Astronautics; and from 2014 he is chair Professor in Shandong University.

His research interests is oriented to different microgrid aspects, including power electronics, distributed energy-storage systems, hierarchical and cooperative control, energy management systems, and optimization of microgrids and islanded minigrids. Prof. Guerrero is an Associate Editor for the IEEE TRANSACTIONS ON POWER ELECTRONICS, the IEEE TRANSACTIONS ON INDUSTRIAL ELECTRONICS, and the IEEE Industrial Electronics Magazine, and an Editor for the IEEE TRANSACTIONS on SMART GRID. He has been Guest Editor of the IEEE TRANSACTIONS ON POWER ELECTRONICS Special Issues: Power Electronics for Wind Energy Conversion and Power Electronics for Microgrids; the IEEE TRANSACTIONS ON INDUSTRIAL ELECTRONICS Special Sections: Uninterruptible Power Supplies systems, Renewable Energy Systems, Distributed Generation and Microgrids, and Industrial Applications and Implementation Issues of the Kalman Filter; and the IEEE TRANSACTIONS on SMART GRID Special Issue on Smart DC Distribution Systems. He was the chair of the Renewable Energy Systems Technical Committee of the IEEE Industrial Electronics Society. In 2014 he was awarded by Thomson Reuters as ISI Highly Cited Researcher, and in 2015 he was elevated as IEEE Fellow for contributions to "distributed power systems and microgrids."